Bull. Chem. Soc. Jpn., 68, 2159—2164(1995)

Volume Study on the Micelle Formation of Local Anesthetic Dibucaine Hydrochloride and Dodecyltrimethylammonium Chloride Mixtures

Michio Yamanaka,* Hitoshi Matsuki,† and Shoji Kaneshina†

Department of Chemistry, Faculty of Science, Kyushu University Ropponmatsu,
Ropponmatsu, Fukuoka 810

†Department of Biological Science and Technology, Faculty of Engineering, The University of Tokushima,
Minamijosanjima-cho, Tokushima 770

(Received January 5, 1995)

Densities of aqueous solutions of mixtures of dibucaine hydrochloride (DCHC), a local anesthetic, and dodecyltrimethylammonium chloride (DTAC) were measured as functions of total molality. The apparent molar volumes of the mixtures were calculated from the density data. The molar volumes in the monomeric and micellar states were evaluated from the dependence of the apparent molar volume on the total molality. The critical micelle concentration (cmc) of the mixtures was determined from the break point of the apparent molar volume vs. the total molality curves, while the micellar composition was evaluated from the dependence of the cmc on the mole fraction of DTAC in the mixture. The composition diagram of micellization has a swollen cigar shape, slightly distorted in the composition range near the DTAC component; such a distortion indicates slightly non-ideal mixing between the hydrophobic groups of DCHC and DTAC molecules in the micelle. However, the molar volume of micellar state varies depending upon the micellar composition along a straight line connecting the molar volumes of DCHC and DTAC. Moreover, the volume of micelle formation is smaller for DCHC, which has larger monomer and micellar volumes than DTAC, and increases linearly with increasing DTAC composition in the micelle. Therefore, the bulky structure of the hydrophobic part of the DCHC molecule affects both the miscibility and the volume behavior in the DCHC–DTAC mixed micelles.

Local anesthetics are amphiphilic and some of them behave like surfactants in water.[1—7] In a preceding paper,[8] the surface adsorption and volume behavior of the hydrochloride salts of local anesthetics were studied by measuring the surface tension and density of their aqueous solutions. It was shown that some local anesthetics form micelles in aqueous solutions and adsorb strongly at the solution surface. A correlation between the surface activity and the anesthetic action of the local anesthetics was suggested. Further, it is known that the interactions between anesthetic molecules and cell membranes are important for the anesthetic action, and that one key parameter characterizing the interactions is the partial molar volume.[9—13] Therefore, in order to elucidate the molecular mechanism of the anesthetic action, it is necessary to accumulate further thermodynamic information on the molecular interactions between anesthetics and model biomembranes.

Recently, we have investigated the relation between the volume behavior of mixed micelles and the miscibility of the surfactants for binary surfactant systems by measuring the density of the aqueous solutions.[14,15] It would be interesting to know the effect of the molecular structure characteristic of a local anesthetic on the volume behavior of the mixed micelles and their miscibility in a mixed system of a local anesthetic and a surfactant. Therefore, in the present work, we use dibucaine hydrochloride (DCHC), which forms micelles in water, and dodecyltrimethylammonium chloride (DTAC). The molar volumes and the compositions of the mixed micelles of DCHC and DTAC are obtained thermodynamically from the density measurements of aqueous solutions of mixtures of DCHC and DTAC. The relationship between the volume behavior and the miscibility in the mixed micelle is discussed.

Experimental

Materials. Dibucaine hydrochloride (DCHC), purchased from Sigma Chemical Co., was recrystallized twice with acetone. Dodecyltrimethylammonium chloride (DTAC), purchased from Tokyo Kasei Kogyo Co., Ltd., was recrystallized six times by using a mixture of acetone and ethanol. The water was distilled twice; in the second step, small amounts of potassium permanganate and potassium hydroxide were added. The molecular structure of dibucaine hydrochloride is shown in Fig. 1: it has a butoxylated quinoline ring, an amide group, and a diethylamino group. Since

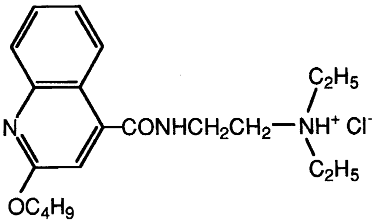

Fig. 1. Molecular structure of dibucaine hydrochloride.

the pK_a values of quinoline and triethylamine are 4.97 and 10.72, respectively,[16] the protonation occurs only on the nitrogen atom of the diethylamino group under the present experimental conditions. Thus, the protonated diethylamino group of DCHC acts as a hydrophilic group. Moreover, DCHC is assumed to be a strong electrolyte.[8]

Method. The density, ρ, of the aqueous solution of DCHC (component 1) and DTAC (component 2) mixture was measured as a function of the total molality m_t and the composition, X_2, of the mixture at 25±0.001 °C under atmospheric pressure by using a vibrating tube density meter (Anton Paar DMA 60/602). m_t and X_2 are defined as

$$m_t = m_1 + m_2 \tag{1}$$

and

$$X_2 = m_2/m_t, \tag{2}$$

where m_i is the molality of component i. The experimental error in the density was within ± 0.001 kg m^{-3}.

Results and Discussion

The experimental results of the densities, ρ, of aqueous solutions of the DCHC–DTAC mixtures are listed in Table 1. The data for the pure system of DTAC are reproduced from our recent paper.[15] The apparent molar volume, ϕ_t, of the mixtures at constant composition was calculated from the density data by using

$$\phi_t = (1/\rho - 1/\rho_w)/m_t + M/\rho, \tag{3}$$

where ρ_w is the density of pure water, M the mean molar mass of the mixtures defined by

$$M = M_1X_1 + M_2X_2, \tag{4}$$

where M_i is the molar mass of component i. The ϕ_t vs. m_t curves are drawn in Fig. 2. The curve of DCHC (X_2=0) coincides with that in the preceding paper.[8] ϕ_t for DTAC (X_2=1.0) is almost constant below the cmc, begins to increase at the cmc, and approaches asymptotically to a value at high concentration with increasing m_t. On the other hand, ϕ_t for DCHC (X_2=0) decreases slightly with increasing m_t below the cmc, and increases gradually above the cmc. Although ϕ_t of DCHC is greater than that of DTAC, it doesn't seem to be affected strongly by the formation of the micelles. The shape of the curves for mixtures changes gradually with composition between the shape for DCHC and that for DTAC. By the least-squares method, the following equations were fitted to the ϕ_t values:

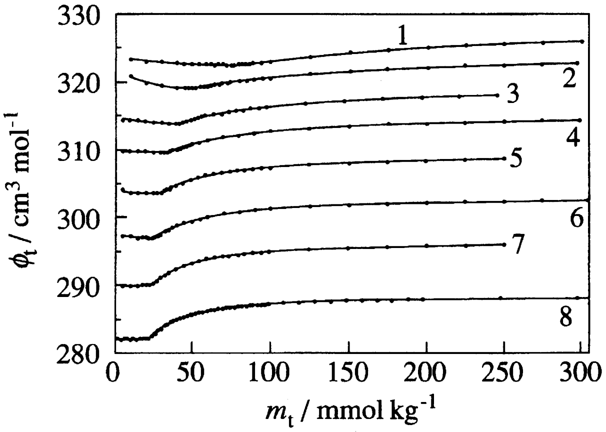

Fig. 2. Apparent molar volume vs. total molality curves at constant composition: X_2=(1) 0, (2) 0.0952, (3) 0.2032, (4) 0.3256, (5) 0.4684, (6) 0.6312, (7) 0.7962, (8) 1.

$$\phi_t = A_0 + A_1m_t + A_2(m_t)^2 + A_3(m_t)^3 \quad (m_t < C_t) \tag{5}$$

and

$$\phi_t = B_0 + B_1/m_t + B_2/(m_t)^2 + B_3/(m_t)^3, \quad (m_t > C_t), \tag{6}$$

where C_t is the critical micelle concentration (cmc) and A_i (i=0, 1, and 2) and B_j (j=0, 1, 2, and 3) are parameters chosen to give the best fit; these are shown in Table 2.

From the concentration dependence of the apparent molar volume of the mixtures, the molar volumes of the mixtures in the monomeric and micellar states were obtained by using the following equations:[14]

$$V_t^W = X_1V_1^W + X_2V_2^W = \partial(m_t\phi_t)/\partial m_t \quad (m_t < C_t) \tag{7}$$

and

$$V^M/N_t^M = \partial(m_t\phi_t)/\partial m_t, \quad (m_t \gg C_t), \tag{8}$$

where V_i^W (i=1 and 2) is the partial molar volume of monomeric component i, V^M the molar volume of the micelle, N_t^M ($=N_1^M + N_2^M$) the number of solute molecules in the micelle, and C_t the cmc. The molar volume of the micelle and the number of solute molecules in the micelle are defined as the excess quantities with reference to the dividing spherical interface which is located around the micelle so as to make the excess number of water molecules be zero.[17] Practically, we evaluated $\partial(m_t\phi_t)/\partial m_t$ by using the following equations:

$$\partial(m_t\phi_t)/\partial m_t = A_0 + 2A_1m_t + 3A_2(m_t)^2 + 4A_3(m_t)^3 \quad (m_t < C_t) \tag{9}$$

and

$$\partial(m_t\phi_t)/\partial m_t = B_0 - B_2(m_t)^{-2} - 2B_3(m_t)^{-3} \quad (m_t > C_t). \tag{10}$$

In Fig. 3, $\partial(m_t\phi_t)/\partial m_t$ is shown as a function of m_t. The $\partial(m_t\phi_t)/\partial m_t$ vs. m_t curves show a discon-

Table 1. Experimental Densities for Aqueous Solutions of DCHC–DTAC Mixtures

$\frac{m_t}{\mathrm{mmol\,kg^{-1}}}$	$\frac{\rho}{\mathrm{kg\,m^{-3}}}$	$\frac{m_t}{\mathrm{mmol\,kg^{-1}}}$	$\frac{\rho}{\mathrm{kg\,m^{-3}}}$	$\frac{m_t}{\mathrm{mmol\,kg^{-1}}}$	$\frac{\rho}{\mathrm{kg\,m^{-3}}}$
$X_2=0$					
0	997.045	67.010	1000.863	100.184	1002.651
9.947	997.615	69.881	1001.024	125.473	1003.926
20.124	998.200	72.449	1001.170	150.673	1005.156
30.440	998.789	75.440	1001.337	175.428	1006.341
40.114	999.340	77.315	1001.440	200.576	1007.529
45.032	999.623	79.931	1001.578	225.352	1008.676
49.868	999.898	82.087	1001.699	250.067	1009.802
54.852	1000.179	85.063	1001.864	275.110	1010.931
59.466	1000.440	87.386	1001.991	300.760	1012.059
62.318	1000.598	89.459	1002.093		
64.662	1000.734	94.740	1002.368		
$X_2=0.0952$					
9.864	997.526	60.387	1000.030	95.818	1001.624
19.930	998.035	62.687	1000.134	100.510	1001.832
29.856	998.533	65.001	1000.241	125.499	1002.909
40.121	999.049	67.997	1000.378	150.679	1003.969
45.418	999.308	69.704	1000.454	174.888	1004.973
48.146	999.446	73.077	1000.610	200.438	1006.010
50.196	999.546	75.086	1000.697	224.860	1006.981
52.826	999.673	80.673	1000.950	250.283	1007.983
55.344	999.787	85.181	1001.156	274.961	1008.936
57.975	999.914	90.043	1001.367	297.980	1009.816
$X_2=0.2032$					
4.917	997.255	46.565	999.017	83.088	1000.397
9.616	997.456	49.188	999.119	88.017	1000.570
14.591	997.668	51.597	999.213	93.132	1000.760
19.690	997.888	53.993	999.304	98.052	1000.937
24.668	998.102	56.482	999.394	122.278	1001.808
29.880	998.326	58.995	999.490	147.381	1002.684
34.418	998.524	63.865	999.678	171.790	1003.521
39.461	998.739	69.077	999.878	196.779	1004.361
41.679	998.827	74.032	1000.059	221.108	1005.167
44.032	998.919	78.445	1000.220	245.253	1005.972
$X_2=0.3256$					
5.065	997.213	40.328	998.360	90.237	999.727
9.820	997.370	42.368	998.417	100.135	999.989
14.772	997.535	43.680	998.452	124.909	1000.636
19.697	997.697	46.346	998.528	149.993	1001.279
24.567	997.858	48.406	998.585	175.042	1001.908
29.674	998.027	50.162	998.636	199.826	1002.525
31.701	998.093	54.969	998.775	224.340	1003.119
33.716	998.159	60.099	998.914	250.103	1003.741
35.563	998.217	70.131	999.188	274.860	1004.319
37.330	998.266	80.145	999.460	299.410	1004.896
$X_2=0.4684$					
4.897	997.154	36.676	997.841	84.212	998.642
9.953	997.271	39.628	997.899	89.279	998.722
15.097	997.387	43.881	997.971	94.487	998.810
19.995	997.498	49.441	998.064	99.853	998.898
24.919	997.609	54.233	998.143	124.506	999.283
27.006	997.655	58.990	998.217	149.765	999.678
30.279	997.732	64.355	998.311	174.540	1000.059
31.507	997.746	69.545	998.399	199.239	1000.429
33.099	997.776	74.634	998.486	224.863	1000.809
35.186	997.821	79.327	998.560	249.842	1001.173

Table 1. (Continued)

$\frac{m_t}{\mathrm{mmol\,kg^{-1}}}$	$\frac{\rho}{\mathrm{kg\,m^{-3}}}$	$\frac{m_t}{\mathrm{mmol\,kg^{-1}}}$	$\frac{\rho}{\mathrm{kg\,m^{-3}}}$	$\frac{m_t}{\mathrm{mmol\,kg^{-1}}}$	$\frac{\rho}{\mathrm{kg\,m^{-3}}}$
X_2=0.6312					
5.160	997.098	32.713	997.357	90.506	997.615
10.139	997.149	34.629	997.366	100.300	997.654
15.131	997.204	37.137	997.377	125.330	997.756
17.542	997.228	40.116	997.393	150.197	997.858
20.068	997.255	44.892	997.414	174.963	997.957
22.052	997.277	50.483	997.450	199.675	998.056
24.092	997.298	55.313	997.470	224.818	998.150
25.859	997.315	60.296	997.491	249.666	998.246
27.902	997.331	70.643	997.533	274.341	998.337
29.594	997.340	80.537	997.575	304.770	998.461
X_2=0.7962					
5.097	997.038	34.844	996.929	83.799	996.539
10.076	997.031	39.468	996.892	89.442	996.492
14.765	997.024	44.938	996.845	94.899	996.451
17.551	997.018	50.032	996.806	99.555	996.413
20.022	997.014	54.668	996.769	124.832	996.215
22.330	997.010	59.748	996.727	149.574	996.028
24.955	996.999	64.997	996.684	174.819	995.840
27.216	996.985	70.276	996.643	199.868	995.654
29.711	996.967	74.244	996.615	225.057	995.473
32.451	996.949	79.772	996.570	249.983	995.298
X_2=1					
1.994	997.011	49.287	996.036	108.734	994.666
4.004	996.976	50.037	996.018	118.682	994.445
5.994	996.941	52.332	995.963	128.699	994.222
7.988	996.907	55.009	995.901	138.404	994.012
9.968	996.873	57.400	995.849	148.642	993.784
11.976	996.838	59.915	995.789	158.633	993.566
13.982	996.805	62.650	995.721	168.554	993.348
15.967	996.771	64.997	995.669	178.026	993.146
18.032	996.734	67.416	995.611	188.711	992.917
19.934	996.702	69.895	995.555	198.070	992.715
22.019	996.665	72.580	995.492	247.396	991.682
24.006	996.624	75.027	995.435	297.570	990.661
26.049	996.576	77.486	995.380	346.779	989.688
27.976	996.531	79.991	995.319	396.561	988.725
29.925	996.487	82.619	995.260	446.818	987.781
32.090	996.434	85.193	995.203	496.966	986.864
33.960	996.389	87.555	995.151	543.149	986.034
35.920	996.343	89.584	995.103	597.880	985.078
38.029	996.294	92.472	995.037	645.867	984.260
39.920	996.250	95.111	994.981	695.690	983.437
42.377	996.195	97.397	994.929	747.305	982.606
45.005	996.134	98.743	994.893	797.451	981.805
47.494	996.075	99.445	994.878	848.641	981.031

tinuous change associated with the micelle formation. $\partial(m_\mathrm{t}\phi_\mathrm{t})/\partial m_\mathrm{t}$ for DCHC in the concentration range above the cmc increases gradually with increasing m_t, while that for DTAC is almost constant, perhaps because DCHC cooperates less in the micelle formation, since the structure of the hydrophobic part of the DCHC molecule is bulky and the number of molecules in the DCHC micelle is low.[18—21] Moreover, although the value of $\partial(m_\mathrm{t}\phi_\mathrm{t})/\partial m_\mathrm{t}$ is larger for the mixture at lower X_2, the magnitude of the discontinuous change at the cmc becomes smaller.

In Fig. 4, V_t^W at the cmc and $V^\mathrm{M}/N_\mathrm{t}^\mathrm{M}$ at 250 mmol kg^{-1} are plotted against the composition X_2. Since X_2 is identical with the monomer composition X_2^W at m_t below the cmc and can be assumed to be the micellar composition X_2^M at sufficiently high m_t above the cmc, the curves are regarded as the V_t^W vs. X_2^W and $V^\mathrm{M}/N_\mathrm{t}^\mathrm{M}$ vs. X_2^M curves. We can find that both of V_t^W and $V^\mathrm{M}/N_\mathrm{t}^\mathrm{M}$ change linearly between their values for single components. Similar results have

Table 2. Fitting Parameters of the ϕ_t vs. m_t

X_2	0	0.0952	0.2032	0.3256	0.4684	0.6312	0.7962	1
$\frac{A_0}{\text{cm}^3\,\text{mol}^{-1}}$	323.58	320.59	314.40	309.91	304.20	297.64	289.74	282.02
$\frac{10^2 A_1}{(\text{cm}^3\,\text{mol}^{-1})(\text{mmol kg}^{-1})^{-1}}$	−3.7399	−5.4872	−0.26887	−1.6610	−6.9685	−4.7164	0.28223	0.31719
$\frac{10^3 A_2}{(\text{cm}^3\,\text{mol}^{-1})(\text{mmol kg}^{-1})^{-2}}$	0.44115	0.48774	−0.85362	0.19798	2.7660	0.71758	0.38994	0.043769
$\frac{10^5 A_3}{(\text{cm}^3\,\text{mol}^{-1})(\text{mmol kg}^{-1})^{-3}}$	−0.18118		1.0804		−3.8034	0.060951		
$\frac{B_0}{\text{cm}^3\,\text{mol}^{-1}}$	327.50	324.31	319.51	315.22	309.47	303.18	296.53	288.71
$\frac{10^{-2} B_1}{(\text{cm}^3\,\text{mol}^{-1})(\text{mmol kg}^{-1})}$	−5.5316	−5.2013	−4.1624	−2.8250	−2.1827	−1.9970	−1.3792	−1.5321
$\frac{10^{-4} B_2}{(\text{cm}^3\,\text{mol}^{-1})(\text{mmol kg}^{-1})^2}$	1.1335	1.5771	1.0622	0.24280	0.060447	0.051066	−0.2.1161	0.0063262
$\frac{10^{-5} B_3}{(\text{cm}^3\,\text{mol}^{-1})(\text{mmol kg}^{-1})^3}$		−1.4733	−1.2917	0.22658	0.21154	0.12601	0.40786	

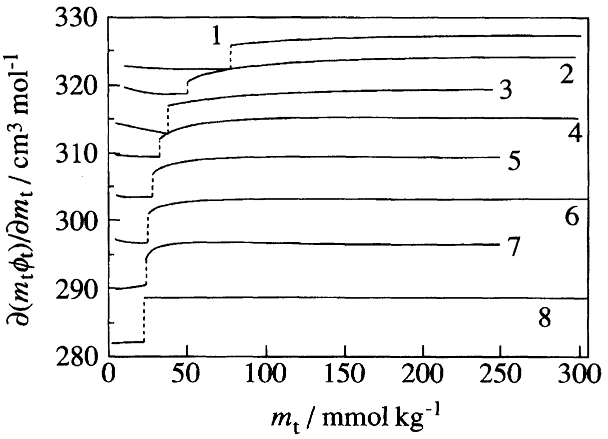

Fig. 3. Partial derivative of $m_t\phi_t$ with respect to total molality vs. total molality curves at constant composition: X_2=(1) 0, (2) 0.0952, (3) 0.2032, (4) 0.3256, (5) 0.4684, (6) 0.6312, (7) 0.7962, (8) 1.

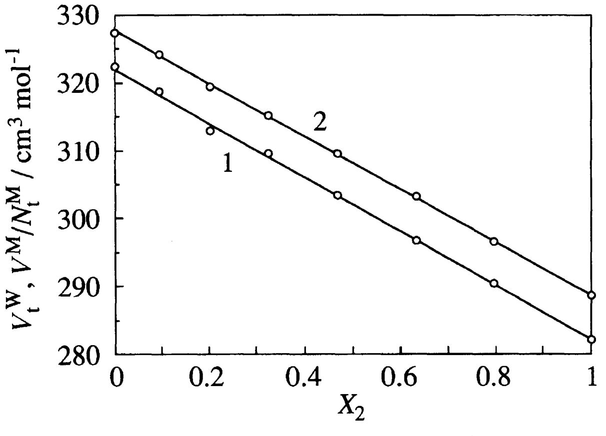

Fig. 4. Molar volumes of monomer (V_t^W) and micelle (V^M/N_t^M) vs. composition curves: (1) V_t^W, (2) V_M/N_t^M.

been obtained for the mixtures of decyltrimethylammonium bromide (DeTAB)–dodecyltrimethylammonium bromide (DTAB)[14] and DTAB–DTAC.[15]

Next, we will consider the miscibility of DCHC molecules with DTAC molecules in the mixed micelle. This is performed by drawing the composition diagram of micellization (CDM)[22] which consists of the C_t vs. X_2 and C_t vs. micellar composition, X_2^M ($=N_2^M/N_t^M$), curves. The cmc value, C_t, of the mixtures was obtained from the intersection of the ϕ_t vs. m_t curves below and above the cmc. In Fig. 5, the C_t values are plotted against X_2. It is found that the cmc of the mixtures are lowered below the line connecting the cmc values of DCHC and DTAC and the C_t vs. X_2 curve is concave upward. Applying

$$X_2^M = X_2 - 2(X_1X_2/C_t)(\partial C_t/\partial X_2)_{T,p} \tag{11}$$

to the C_t vs. X_2 curve, we evaluated the micellar composition X_2^M.[14,17] In Fig. 5, the C_t values are plotted

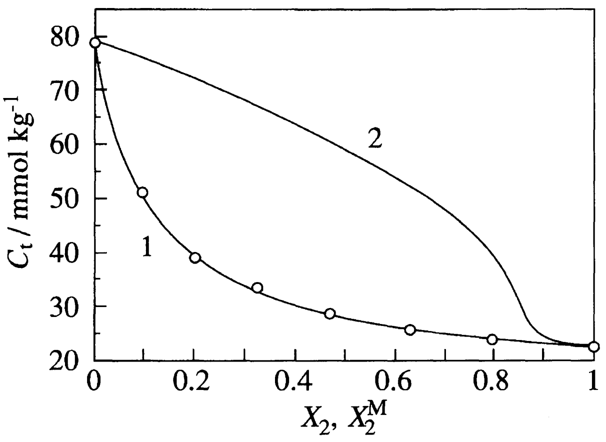

Fig. 5. Critical micelle concentration vs. composition curves: (1) C_t vs. X_2, (2) C_t vs. X_2^M.

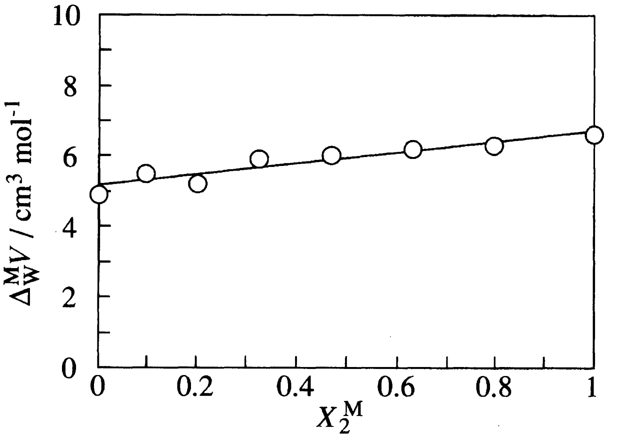

Fig. 6. Volume of micelle formation vs. micellar composition curve.

against X_2^M. The region surrounded by the curves has a swollen cigar shape distorted slightly in the composition range near $X_2=1$. This fact may indicate the slightly non-ideal mixing of the hydrophobic groups of DCHC and DTAC molecules in the micelle. However, this non-ideal mixing doesn't affect the micellar volume, which, as seen in Fig. 4, varies linearly with X_2^M between the values for each component of the DCHC–DTAC system.

Finally, let us calculate the volume of micelle formation, $\Delta_W^M V$, by using[14,17]

$$\Delta_W^M V = V^M/N_t^M - (X_1^M V_1^W + X_2^M V_2^W). \qquad (12)$$

The calculated values of $\Delta_W^M V$ are plotted against X_2^M in Fig. 6. Although DCHC has greater values of the molar volumes in both monomeric and micellar states than DTAC, the value of $\Delta_W^M V$ is smaller for DCHC than for DTAC and increases linearly with X_2^M. Therefore, we may conclude that the bulky structure of the hydrophobic part of DCHC molecule has important effects on the miscibility and the volume behavior in the mixed micelle.

The present work was supported by Grant-in-Aid for Scientific Research (C) No. 05640657 from the Ministry of Education, Science and Culture.

References

1) D. Hellenbrecht, B. Lemmer, G. Wiethold, and H. Grobecker, *Naunyn-Schmiedeberg's Arch. Pharmacol.*, **277**, 211 (1973).

2) H. -C. Lin, I. Ueda, S. H. Lin, D. D. Shieh, H. Kamaya, and H. Eyring, *Biochim. Biophys. Acta*, **598**, 51 (1980).

3) R. C. Srivastava, R. K. Sharma, R. Srinivasan, and S. B. Bhise, *J. Colloid Interface Sci.*, **94**, 456 (1983).

4) D. Attwood and A. T. Florence, "Surfactant Systems," Chapman and Hall, London (1983), Chap. 4.

5) D. Attwood and P. Fletcher, *J. Pharm. Parmacol.*, **38**, 494 (1986).

6) M. Tomoaia-Cotisel and D. A. Cadenhead, *Langmuir*, **7**, 964 (1991).

7) K. J. Miller, II, S. R. Goodwin, G. B. Westermann-Clark, and D. O. Shah, *Langmuir*, **9**, 105 (1993).

8) H. Matsuki, S. Hashimoto, S. Kaneshina, and M. Yamanaka, *Langmuir*, **10**, 1882 (1994).

9) Y. Kita, L. J. Bennet, and K. W. Miller, *Biochim. Biophys. Acta*, **647**, 130 (1981).

10) Y. Kita and K. W. Miller, *Biochemistry*, **21**, 2840 (1982).

11) T. Mori, N. Matubayasi, and I. Ueda, *Mol. Pharmacol.*, **25**, 123 (1984).

12) M. Iqbal and R. E. Verrall, *Can. J. Chem.*, **67**, 727 (1989).

13) J. J. Ramsden, *J. Phys. Chem.*, **97**, 4479 (1993).

14) M. Yamanaka and S. Kaneshina, *J. Solution Chem.*, **19**, 729 (1990).

15) M. Yamanaka and S. Kaneshina, *J. Solution Chem.*, **20**, 1159 (1991).

16) "Kagakubenran Kisohen," Maruzen, Tokyo (1984), Vol. II, p. 339.

17) K. Motomura, M. Yamanaka, and M. Aratono, *Colloid Polym. Sci.*, **262**, 948 (1984).

18) R. Jaenicke, *Kolloid. Z.*, **212**, 36 (1966).

19) E. M. Johnson and D. B. Ludlum, *Biochem. Pharmacol.*, **18**, 2675 (1969).

20) D. Attwood and R. Natarajan, *J. Pharm. Pharmacol.*, **35**, 317 (1983).

21) D. Attwood and P. Fletcher, *J. Pharm. Pharmacol.*, **38**, 494 (1986).

22) M. Yamanaka, H. Matsuki, N. Ikeda, M. Aratono, and K. Motomura, *Langmuir*, **10**, 2950 (1994).